

Visualizing tmRNA Entry into a Stalled Ribosome

Mikel Valle,^{1*} Reynald Gillet,^{2*} Sukhjit Kaur,¹ Anke Henne,³
V. Ramakrishnan,^{2†} Joachim Frank^{1,4†}

Various alternative hypotheses have been proposed to explain the signal content of carotenoid-dependent ornaments (2–5). The relative importance of carotenoid acquisition per se, as influenced by foraging efficiency (24, 25), parasite effects on gut absorption (26), energetic constraints (27), and carotenoid utilization for immune function, in determining the expression of sexual ornaments remains to be seen. However, our results show that immune function can be limited by carotenoid availability in a species with carotenoid-dependent ornamentation and suggest that immunocompetence is one trait that is revealed by the expression of such signals.

References and Notes

1. M. Andersson, *Sexual Selection* (Princeton Univ. Press, Princeton, NJ, 1994).
2. G. E. Hill, *Am. Nat.* **154**, 589 (1999).
3. V. A. Olson, I. P. F. Owens, *Trends Ecol. Evol.* **13**, 510 (1998).
4. A. P. Möller *et al.*, *Avian Poul. Biol. Rev.* **11**, 37 (2000).
5. J. Hudon, *Auk* **111**, 218 (1994).
6. A. Zahavi, *J. Theor. Biol.* **53**, 205 (1975).
7. A. Grafen, *J. Theor. Biol.* **144**, 517 (1990).
8. B. P. Chew, *Anim. Feed Sci. Tech.* **59**, 103 (1996).
9. W. Stahl, H. Sies, in *Antioxidant Food Supplements in Human Health*, L. Packer, M. Hiramatsu, T. Yoshikawa, Eds. (Academic Press, San Diego, CA, 1999), pp. 183–202.
10. G. A. Lozano, *Oikos* **70**, 309 (1994).
11. T. von Schantz, S. Bensch, M. Grahn, D. Hasselquist, H. Wittzell, *Proc. R. Soc. Lond. Ser. B* **266**, 1 (1999).
12. Materials and methods are available as supporting material on Science Online.
13. K. J. McGraw, E. Adkins-Regan, R. S. Parker, *Comp. Biochem. Physiol. B* **132**, 811 (2002).
14. K. J. McGraw, G. E. Hill, R. Stradi, R. S. Parker, *Physiol. Biochem. Zool.* **74**, 843 (2001).
15. N. Burley, C. B. Coopersmith, *Ethology* **76**, 133 (1987).
16. C. H. De Kogel, H. J. Prijs, *Anim. Behav.* **51**, 699 (1996).
17. T. R. Birkhead, F. Fletcher, E. J. Pellatt, *Proc. R. Soc. Lond. Ser. B* **266**, 385 (1999).
18. A. M. Houtman, *Proc. R. Soc. Lond. Ser. B* **249**, 3 (1992).
19. S. A. Collins, C. Hubbard, A. M. Houtman, *Behav. Ecol. Sociobiol.* **35**, 21 (1994).
20. S. A. Collins, C. Ten Cate, *Anim. Behav.* **52**, 105 (1996).
21. F. McCorkle Jr., I. Olah, B. Glick, *Poult. Sci.* **59**, 616 (1980).
22. G. Gonzalez *et al.*, *J. Anim. Ecol.* **68**, 1225 (1999).
23. W. D. Hamilton, M. Zuk, *Science* **218**, 384 (1982).
24. A. Kodric-Brown, *Behav. Ecol. Sociobiol.* **25**, 393 (1989).
25. G. E. Hill, *Auk* **109**, 1 (1992).
26. K. J. McGraw, G. E. Hill, *Proc. R. Soc. Lond. Ser. B* **267**, 1525 (2000).
27. G. E. Hill, *J. Avian Biol.* **31**, 559 (2000).
28. We thank C. A. Adams, G. Adam, D. Armstrong, J. Barnett, G. L. Devey, J. Freal, A. Kirk, J. Laurie, H. Lepitak, P. Monaghan, and T. Mora for logistical help; K. E. Arnold, M. S. Edwards, M. H. Graham, J. Lindström, F. McPhie, P. Monaghan, R. G. Nager, N. J. Royle, N. Verboven, and two anonymous reviewers for advice about statistical analyses and other comments on the manuscript; Kemin Industries Incorporated (USA) for donating carotenoids; and the Natural Environment Research Council for funding.

Supporting Online Material

www.sciencemag.org/cgi/content/full/300/5616/125/DC1

Materials and Methods
Table S1

7 January 2003; accepted 6 March 2003

Bacterial ribosomes stalled on defective messenger RNAs (mRNAs) are rescued by tmRNA, an ~300-nucleotide-long molecule that functions as both transfer RNA (tRNA) and mRNA. Translation then switches from the defective message to a short open reading frame on tmRNA that tags the defective nascent peptide chain for degradation. However, the mechanism by which tmRNA can enter and move through the ribosome is unknown. We present a cryo-electron microscopy study at ~13 to 15 angstroms of the entry of tmRNA into the ribosome. The structure reveals how tmRNA could move through the ribosome despite its complicated topology and also suggests roles for proteins S1 and SmpB in the function of tmRNA.

During the normal course of protein synthesis, a problem occurs if the ribosome reaches the 3' end of a defective or degraded mRNA

before it encounters a stop codon. This situation has two possible consequences: the ribosome can stall, and the incomplete polypeptide made as a result may be toxic to the cell. In bacteria, both these problems are solved simultaneously by the intervention of an RNA molecule called 10Sa RNA, SsrA, or most commonly, tmRNA, because it incorporates within a single molecule the functions of both tRNA and mRNA (*I–3*). The tmRNA molecule is ~260 to 430 nucleotides long, depending on bacterial species, and contains both a tRNA-like domain (TLD) that can be charged with alanine at its 3' CCA end and an internal stretch of RNA that contains a short open reading frame (ORF). The molecule first

¹Howard Hughes Medical Institute, Wadsworth Center, Health Research, Inc., Empire State Plaza, Albany, NY 12201–0509, USA. ²MRC Laboratory of Molecular Biology, Hills Road, Cambridge CB2 2QH, UK. ³Göttingen Genomics Laboratory, Institute of Microbiology and Genetics, Grisebachstrasse 8, 37077 Göttingen, Germany. ⁴Department of Biomedical Sciences, State University of New York at Albany, Empire State Plaza, Albany, New York 12201–0509, USA.

*These authors contributed equally to this work.
†To whom correspondence should be addressed. E-mail: ramak@mrc-lmb.cam.ac.uk (V.R.); joachim@wadsworth.org (J.F.)

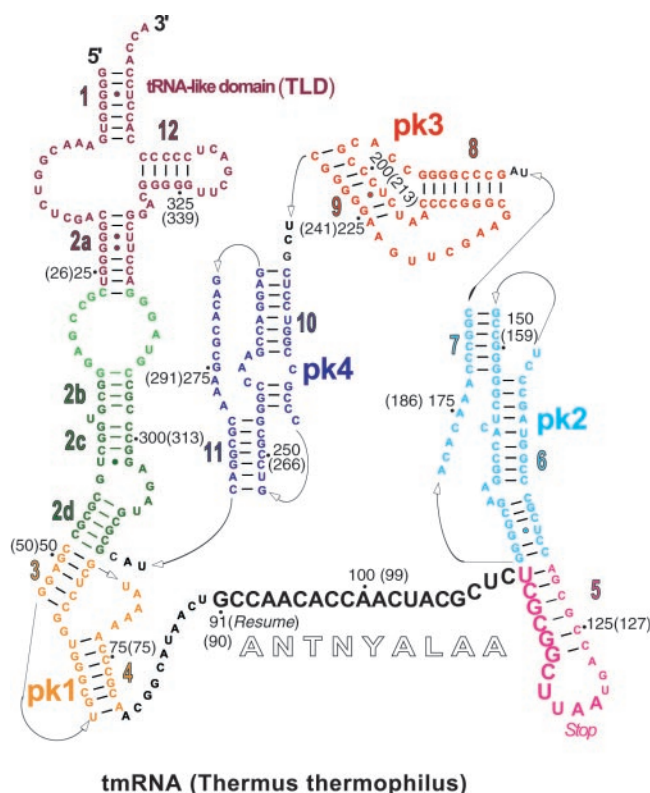


Fig. 1. Secondary structure diagram of tmRNA. Base pairs are linked by lines, whereas GU pairs are represented by dots. The TLD, the four pseudoknots (PK1 to PK4), and helices (numbered from 1 to 12) are shown in the colors that are used to represent these modules in subsequent figures. The nucleotides within the ORF are shown in a larger font. *T. thermophilus* sequence numbers are shown, with the corresponding *E. coli* numbering in parentheses. The figure is adapted from the diagram for *E. coli* on the tmRDB Web site (29, 41).

REPORTS

binds in the A site of the stalled ribosome and allows its alanine to be added to the nascent polypeptide chain through its TLD. After peptidyl transfer, the TLD must translocate to the ribosomal P site. The template for translation is then switched from the original defective mRNA to the ORF of tmRNA, a process termed trans-translation. Normal termination occurs when the stop codon at the end of the ORF is reached. The result is that the stalled ribosome is rescued and the defective protein is tagged for degradation at its C-terminus (4). Apart from acting on defective mRNA, tmRNA has also been implicated in acting on real stop codons or internal mRNA sites (5, 6). However, a recent study shows that the bacterial toxin relE cleaves rare codons on mRNA in the A site

(7), so these cases of tmRNA rescue may also involve truncated mRNAs. Although tmRNA does not have to decode mRNA in the usual way, it has been shown that EF-Tu (elongation factor Tu) and GTP (guanosine triphosphate) bind tmRNA to form a ternary complex as they do with tRNAs (8, 9). However, it has also been reported that EF-Tu cross-links to two different sites on tmRNA (10). Apart from EF-Tu, at least two other proteins have been implicated in tmRNA function. A small protein, SmpB, has been shown to be required for tmRNA-mediated peptide-tagging activity (11), and ribosomal protein S1, which is known to bind single-stranded RNA, has been proposed to be required for tmRNA binding to the ribosome (12).

The secondary structure of tmRNA is well established (13–15). In addition to the TLD and ORF, the molecule typically contains four pseudoknots, PK1 to PK4 (Fig. 1). Because of its function, tmRNA lacks an anticodon stem-loop. This is replaced by an irregular helix, H2, that is broken by an internal loop, followed by a disrupted helix that is connected to the first pseudoknot, PK1. The internal ORF follows PK1 and is partially located within helix H5. It encodes a short hydrophobic peptide that is a suitable substrate for multiple proteases (16). The three other pseudoknots, PK2 to PK4, connect the ORF back to the TLD. In some species, tmRNA is made in two pieces that fold together to produce a similar overall structure (17).

We have determined the structure of a complex of tmRNA with the ribosome by cryo-electron microscopy (cryo-EM). Kirromycin (kir) allows GTP hydrolysis by EF-Tu but stalls the EF-Tu•GDP complex with tRNA on the ribosome before the accommodation of the tRNA into the peptidyl transferase site (18–21). To visualize the analogous state for tmRNA, we formed a complex of the 70S ribosome from *Thermus thermophilus* with initiator tRNA and an mRNA that contains a Shine-Dalgarno sequence and ends with a start codon in the P site. This complex, with no codon in the A site, was reacted with alanylated tmRNA, SmpB, EF-Tu, and GTP in the presence of kirromycin (22). A cryo-EM map at ~13 Å resolution was obtained by single-particle reconstruction (Fig. 2, A and B) (22). Density is clearly present for the 70S ribosome, as it is for the P-site tRNA, whereas the E site is empty. By comparison of the 70S•tmRNA•EF-Tu•GDP•SmpB•kir complex with control 70S, a density attributable to EF-Tu, SmpB, and tmRNA (in red in Fig. 2, A and B) is observed at the entrance of the ribosomal inter-subunit space, between the base of the L7/L12 stalk in the 50S subunit and the decoding site in the 30S subunit. The mass protrudes prominently along the beak of the 30S subunit and forms an arc at the solvent side that reaches the vicinity of the mRNA channel entrance (23, 24).

Along with the secondary structure of tmRNA, the previously known structures of the ternary complex of EF-Tu (25), SmpB (26), the 30S subunit and 70S ribosome-tRNA complex from *T. thermophilus* (27, 28), and the cryo-EM structure of the ternary complex bound to the *Escherichia coli* ribosome (20, 21) allowed us to interpret the cryo-EM density map. In addition, a three-dimensional model in the tmRNA database (tmRDB) (29) was useful in providing model structures of the helices and pseudoknots suitable for fitting into the cryo-EM map as modules. The resulting assignments of these elements within the cryo-EM density map are depicted in the model shown in Fig. 2C. Because a mass shaped like EF-Tu occurs in a

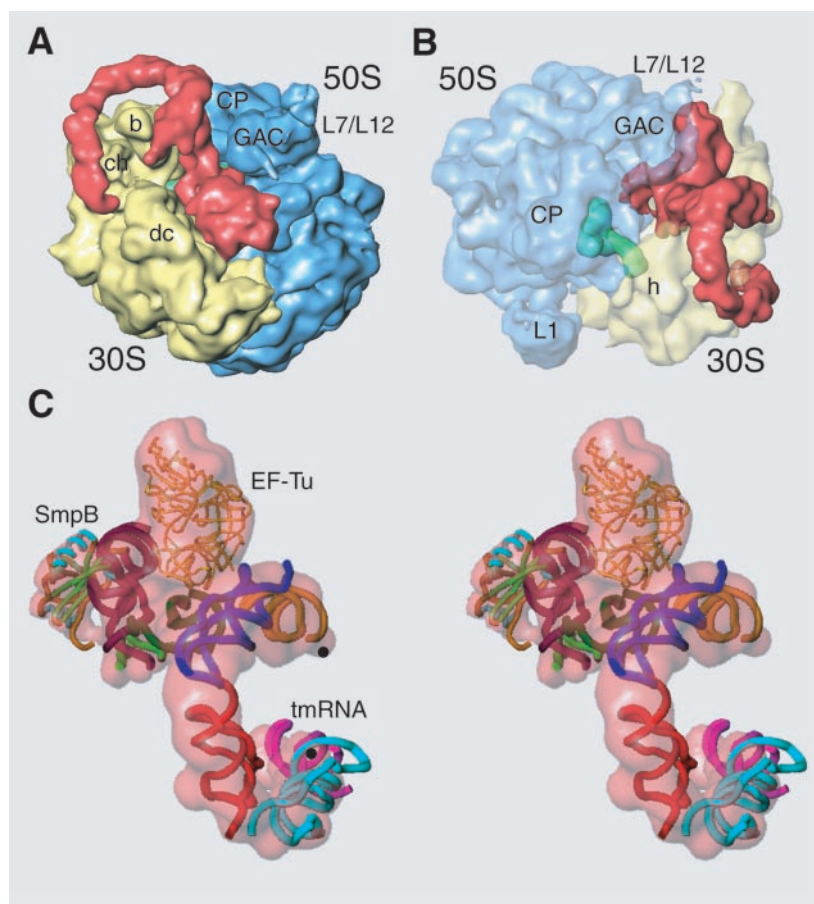


Fig. 2. Model for tmRNA, EF-Tu, and SmpB in the cryo-EM map of 70S ribosome in complex with tmRNA. Cryo-EM map obtained for 70S•tRNA•EF-Tu•tmRNA•SmpB in the presence of GTP and kirromycin (A and B). The 50S subunit is depicted in blue, the 30S subunit in yellow, and the P-site tRNA in green. Semitransparent ribosomal subunits in (B) show the relative position between EF-Tu•tmRNA•SmpB and P-site tRNA. Landmarks on the 50S subunit: L1, stalk of protein L1; CP, central protuberance; L7/L12, stalk of the proteins L7/L12; and GAC, GTPase-associated center. Landmarks on the 30S subunit: h, head; b, beak; dc, decoding center; and ch, entrance of mRNA channel. The density attributable to the EF-Tu•tmRNA•SmpB complex is colored in red and depicted semitransparent in the stereo pair of (C) (orientation as in panel 2B). The docked atomic coordinates are shown in a ribbons representation generated with the programs RIBBONS or Insight. The fitting of the coordinates for EF-Tu•GTP analog [Protein Data Bank (PDB) code 1TTT] (25) and the 3D model for tmRNA (29) did not account for the whole density. The coordinates for SmpB (PDB code 1K8H) (26) were satisfactorily docked in the unexplained region. The ribbon colors for elements of tmRNA model are the same as in the other figures: TLD, burgundy; loop within helix H2, light green; helix H2b-d, dark green; PK1, orange; PK4, dark blue; PK3, red; PK2, light blue; and helix H5, magenta.

location virtually identical to that in the cryo-EM structure of the ternary complex bound to the ribosome (19–21), EF-Tu could readily be placed. This immediately allowed the placement of the TLD into the density, because its contacts with EF-Tu are similar to those of tRNA. However, in tmRNA an increased angle of $\sim 110^\circ$ between the acceptor and “anticodon” arms (rather than the $\sim 90^\circ$ of canonical tRNAs) was predicted by transient electric birefringence data (30). This increased angle is in good agreement with the density obtained in the present work. Although no prior evidence on the role of kirromycin on EF-Tu bound to tmRNA existed, we reasoned that its effect on EF-Tu would be the same as with canonical tRNAs, and this effect indeed is observed. As expected, EF-Tu•GDP is bound to tmRNA by interacting with its acceptor arm, as with tRNAs. This result suggests that, even though tmRNA does not participate in normal decoding of mRNA, GTP hydrolysis by EF-Tu is essential for its function, just as it is for tRNAs. Cross-linking experiments have suggested unusual modes of interaction of EF-Tu with tmRNA, including a second binding site for EF-Tu (10). These interactions are not supported by our model for EF-Tu binding, which is very similar to that of tRNA. However, it is possible that such interactions could occur outside the ribosome.

With the position of the TLD defined, and taking into account the connectivity in both tmRNA’s secondary structure and the cryo-EM density, we could assign all the elements in the tmRNA molecule inside the isolated density (Fig. 2C). Furthermore, after the placement of EF-Tu and tmRNA in the three-dimensional (3D) map, additional density in the vicinity of the acceptor arm of the TLD was still unexplained. This density was assigned to SmpB on the basis of its size, shape, and previous biochemical data showing that the protein interacts with the TLD (31, 32). The NMR structure of SmpB from *Aquifex aeolicus* (26) was positioned into the density in a preferred orientation (Fig. 2C). The position of the docked protein agrees with previous footprinting data as well as mutational analysis, which suggests that the protein interacts with the elbow and the lower portion of TLD through a contact surface that includes the C-terminus of the protein (31, 32). In our interpretation of the cryo-EM map, the protein bridges the TLD and helices H69, H71, and H89 of the 23S rRNA (Fig. 3A), thus enhancing the binding of tmRNA to the ribosome. In the delivery of canonical tRNAs, the interaction of H69 is established with the tRNA itself (20, 21); thus, SmpB seems to complement the TLD to facilitate this contact. The close interactions of SmpB with the 50S subunit and the TLD suggest that SmpB may facilitate GTPase (guanosine triphosphatase) activation by EF-Tu even in

the absence of a normal decoding signal from codon-anticodon interactions. The proposal that two or three copies of SmpB may interact at the same time with tmRNA (33) is not supported by the current maps, but its occurrence cannot be excluded during other stages of trans-translation.

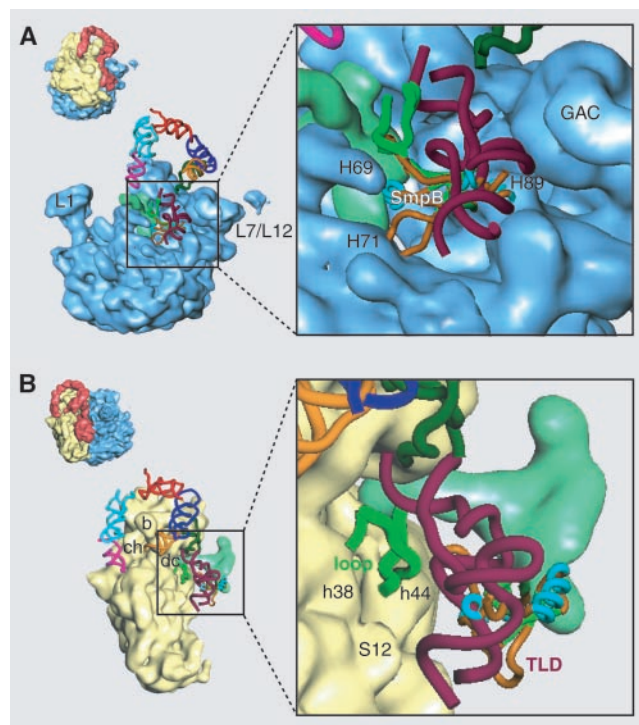
In our model, the TLD interacts with the GTPase-associated center (GAC) in the 50S subunit (Fig. 3A) and with protein S12 in the 30S subunit (Fig. 3B), in a way similar to that of tRNA during the elongation cycle (20, 21). In agreement with a previous suggestion (30), the increased angle of $\sim 110^\circ$ between the acceptor and “anticodon” arms of the TLD places a highly conserved internal loop between helices 2a and 2b deep into the decoding site. It is bound to the vicinity of the tip of helices h44 and h38 from the 16S rRNA of the 30S subunit, with a resulting sharp turn in tmRNA’s structure (Figs. 2C and 3B). It is possible that, independent of a codon, interactions of this region of the tmRNA with the 30S subunit trigger conformational changes in the decoding site and the GTP hydrolysis by EF-Tu, leading to the movement of the TLD into the peptidyl-transferase site. The protein SmpB may also play a role in this process. A direct interaction between H69 of the 50S subunit and elongator tRNA (20, 21) is mediated through SmpB in the case of tmRNA. Because H69 forms an intersubunit bridge with h44 on the 30S subunit close to the decoding site, this interaction may be im-

portant for transmission of the decoding signal to EF-Tu. The rest of helix 2 of tmRNA is redirected along the 30S subunit beak, ending in the fork between the pseudoknots PK1 and PK4 near the top of the beak.

The single-stranded RNA that includes part of the ORF is not visible, but it presumably connects PK1 to helix 5, approximately in the regions labeled with black dots in Fig. 2C. However, it is apparent that in this state, the resume codon of the ORF cannot yet have entered the decoding site in the 30S subunit and will do so only after accommodation of the TLD into the peptidyl-transferase site. The 3’ end of the ORF forms part of the double-stranded helix 5. This part is close to the entrance of the mRNA channel in the 30S subunit (23, 24). However, the tmRNA ternary complex analyzed here is representative of the initial selection step for the TLD. The movements that result from accommodation of the TLD, peptidyl transfer, and translocation of the TLD into the P site will need to pull PK1 and its downstream sequence toward the decoding site to place the resume codon in the correct position for decoding in the A site. It is very likely that in this position, interactions between the highly conserved PK1 downstream region and ribosomal elements are required for the correct positioning of the resume codon in the decoding site and resumption of translation from the ORF.

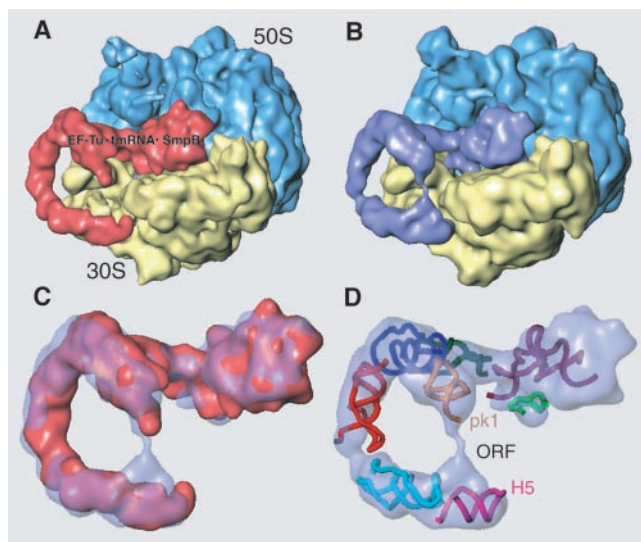
The remaining string of pseudoknots PK4-PK2 and helix 5 form the aforementioned arc that wraps around the beak of the 30S subunit

Fig. 3. Interactions of SmpB•tmRNA with the 70S ribosome. Two different ribosomal orientations are used to illustrate the interactions of SmpB and tmRNA with the 50S subunit (A) and the 30S subunit (B). The orientations are defined by ribosomal thumbnails on the left. Landmarks on the 50S subunit (A): L1, L1 stalk; L7/L12, stalk of proteins L7/L12; GAC, GTPase-associated center; H69, H71, and H89, helices of the 23S rRNA. Labeling on the 30S subunit (B): ch, entrance of the mRNA channel; dc, decoding site; b, beak; loop, RNA loop within helix H2 of tmRNA; TLD, tRNA-like domain of tmRNA; S12, ribosomal protein S12; h44 and h38, the position of those helices from 16S rRNA. Color coding for the tmRNA is as in Fig. 2C. For clarity, EF-Tu is not shown.



REPORTS

Fig. 4. Comparison of maps of tmRNA complexes with and without S1. Cryo-EM maps for the 70S•tRNA•EF-Tu•tmRNA•SmpB complex in the presence (A) and absence (B) of ribosomal protein S1. Different colors for the density attributable to EF-Tu•tmRNA•SmpB are used to allow a comparison in (C), where the purple semitransparent map from (B) is depicted together with the solid red from (A). In the absence of S1 (B) an additional connection is seen between PK1 and helix H5 of the tmRNA (D) that reveals the presence of the folded ORF.



(Figs. 2C and 3B). Those elements are not required for tmRNA function and can be replaced by single-stranded RNA, which suggests that they are involved in stabilizing tmRNA rather than participating directly in its function (34). Our model provides a structural explanation of this finding, because the dispensable pseudoknots PK2 to PK4 form the arc outside the head of the 30S subunit without forming extensive contacts with it. Such an absence of extensive contacts could be required to allow movement of the arc while the ORF and TLD progress inside the ribosome during translation. Nevertheless, the existence of the pseudoknots suggests that they play a role in the presentation of the tmRNA to the ribosome and in helping to orient the ORF and TLD. These pseudoknots are positioned such that, despite their large size, they would not interfere with the subsequent binding of elongation factors and tRNAs. Our model supports the idea that the unwinding of RNA from helix 5 allows movement of the ORF through the ribosome without requiring a large change in the conformation of the rest of tmRNA.

Ribosomal protein S1 is thought to be associated with tmRNA and to be required for tmRNA function (12). Although the 70S complex described was formed in the presence of S1, the protein could not be localized in our map, either on tmRNA or on the 30S subunit. Ribosomal protein S1 was localized in *E. coli* in the shoulder of the 30S subunit (35), which is far away from the position that tmRNA displays in our map. However, it is known that the association of S1 with the ribosome is weak and reversible (36). A separate reconstruction of the identical tmRNA complex in the absence of S1 reveals interesting features (Fig. 4). First, the ternary complex of tmRNA can stably bind ribosomes in the absence of S1 (Fig. 4B). However, in this case, an extension of density from PK1 is now visible, suggesting that a portion of

the single-stranded region including the 5'-end of the ORF is more structured in the absence of S1. By contrast, in the presence of S1 (Fig. 4A) this element cannot be seen, probably because it is unfolded. This difference suggests that S1, without being bound to the ribosome, may play a role in unwinding part of the single-stranded region, thus allowing correct presentation of the ORF. This role would be consistent with prior biochemical evidence showing that S1 can disrupt helical regions in mRNAs (37). Previous UV-induced cross-linking experiments showed the importance of nucleotide U85 from *E. coli* tmRNA in the binding of S1 (12). This nucleotide is situated in the vicinity of the 86 to 88 span, a major determinant for the correct positioning of the resume codon at nucleotides 90 to 92 (38, 39). Similarly, nucleotides in, and upstream of, the resume codon become more accessible to structural probes when S1 binds (40). Regardless of the exact role of S1, it is clear that a stable complex of tmRNA with the ribosome can be formed in the absence of S1, contrary to previous suggestions (12).

The cryo-EM structure presented here addresses a number of interesting questions regarding the functioning of tmRNA. It shows that EF-Tu brings aminoacylated tmRNA to the ribosome in a manner similar to canonical tRNAs. The protein SmpB bridges tmRNA and the 50S subunit. A mimicry of codon-anticodon base pairing between distal parts of tmRNA is shown to be unlikely; rather, an internal loop between helices 2a and 2b is situated close to the decoding site. Protein S1 is potentially involved in unwinding a portion of the ORF. In addition, the cryo-EM structure reveals the locations of the pseudoknots and sheds some light on their individual roles.

References and Notes

1. A. W. Karzai, E. D. Roche, R. T. Sauer, *Nature Struct. Biol.* **7**, 449 (2000).
2. R. Gillet, B. Felden, *Mol. Microbiol.* **42**, 879 (2001).

3. J. H. Withey, D. I. Friedman, *Curr. Opin. Microbiol.* **5**, 154 (2002).
4. K. C. Keiler, P. R. Waller, R. T. Sauer, *Science* **271**, 990 (1996).
5. E. D. Roche, R. T. Sauer, *EMBO J.* **18**, 4579 (1999).
6. ———, *J. Biol. Chem.* **276**, 28509 (2001).
7. K. Pedersen et al., *Cell* **112**, 113 (2003).
8. J. Rudinger-Thirion, R. Giege, B. Felden, *RNA* **5**, 989 (1999).
9. S. Barends, J. Wower, B. Kraal, *Biochemistry* **39**, 2652 (2000).
10. M. I. Zvereva et al., *J. Biol. Chem.* **276**, 47702 (2001).
11. A. W. Karzai, M. M. Susskind, R. T. Sauer, *EMBO J.* **18**, 3793 (1999).
12. I. K. Wower, C. W. Zwieb, S. A. Guven, J. Wower, *EMBO J.* **19**, 6612 (2000).
13. K. P. Williams, D. P. Bartel, *RNA* **2**, 1306 (1996).
14. C. Zwieb, I. Wower, J. Wower, *Nucleic Acids Res.* **27**, 2063 (1999).
15. B. Felden et al., *RNA* **3**, 89 (1997).
16. S. Gottesman, E. Roche, Y. Zhou, R. T. Sauer, *Genes Dev.* **12**, 1338 (1998).
17. K. C. Keiler, L. Shapiro, K. P. Williams, *Proc. Natl. Acad. Sci. U.S.A.* **97**, 7778 (2000).
18. M. V. Rodnina, R. Fricke, L. Kuhn, W. Wintermeyer, *EMBO J.* **14**, 2613 (1995).
19. H. Stark et al., *Nature* **389**, 403 (1997).
20. M. Valle et al., *EMBO J.* **21**, 3557 (2002).
21. H. Stark et al., *Nature Struct. Biol.* **9**, 849 (2002).
22. See Supporting Online Material.
23. J. Frank et al., *Biochem. Cell Biol.* **73**, 757 (1995).
24. G. Z. Yusupova, M. M. Yusupov, J. H. Cate, H. F. Noller, *Cell* **106**, 233 (2001).
25. P. Nissen et al., *Science* **270**, 1464 (1995).
26. G. Dong, J. Nowakowski, D. W. Hoffman, *EMBO J.* **21**, 1845 (2002).
27. B. T. Wimberly et al., *Nature* **407**, 327 (2000).
28. M. M. Yusupov et al., *Science* **292**, 883 (2001).
29. B. Knudsen, J. Wower, C. Zwieb, J. Gorodkin, *Nucleic Acids Res.* **29**, 171 (2001).
30. S. M. Stagg, A. A. Frazer-Abel, P. J. Hagerman, S. C. Harvey, *J. Mol. Biol.* **309**, 727 (2001).
31. S. Barends, A. W. Karzai, R. T. Sauer, J. Wower, B. Kraal, *J. Mol. Biol.* **314**, 9 (2001).
32. K. Hanawa-Suetsugu, M. Takagi, H. Inokuchi, H. Himeno, A. Muto, *Nucleic Acids Res.* **30**, 1620 (2002).
33. J. Wower, C. W. Zwieb, D. W. Hoffman, I. K. Wower, *Biochemistry* **41**, 8826 (2002).
34. N. Nameki, T. Tadaki, H. Himeno, A. Muto, *FEBS Lett.* **470**, 345 (2000).
35. J. Sengupta, R. K. Agrawal, J. Frank, *Proc. Natl. Acad. Sci. U.S.A.* **98**, 11991 (2001).
36. M. Laughrea, P. B. Moore, *J. Mol. Biol.* **112**, 399 (1977).
37. D. G. Bear et al., *Proc. Natl. Acad. Sci. U.S.A.* **73**, 1824 (1976).
38. K. P. Williams, K. A. Martindale, D. P. Bartel, *EMBO J.* **18**, 5423 (1999).
39. S. Lee, M. Ishii, T. Tadaki, A. Muto, H. Himeno, *RNA* **7**, 999 (2001).
40. V. Bordeau, B. Felden, *Biochimie* **84**, 723 (2002).
41. The tmRDB Web site, <http://psyche.uthct.edu/dbs/tmRDB/tmRDB.html>.
42. We thank T. Ueda for a clone of AlaRS, and M. Tarry, F. Murphy, and D. Brodersen for purified 70S ribosomes, EF-Tu, and S1, respectively. We thank R. Grassucci for taking micrographs of a control, M. Watters for assistance with the illustrations, and A. Verschoor for helpful comments on the manuscript. V.R. was supported by grants from the Medical Research Council (UK), GM 44973 from NIH, and the Human Frontier Science Program. R.G. was the recipient of an EMBO postdoctoral fellowship. J.F. was supported by Howard Hughes Medical Institute and grants GM29169 and GM55440 from NIH.

Supporting Online Material

www.sciencemag.org/cgi/content/full/300/5616/1271/DC1

Materials and Methods

Fig. S1

References

20 December 2002; accepted 13 February 2003